Supplemental Methods

Dynamic-clamp and models

Artificial T currents used in Supplemental Figure 3 were simulated by an Hodgkin-Huxley-like model

$I_T = G_{Ca}\, m^2\, h\, (V-V_{Ca})$.

where G_{Ca} is the maximal conductance, V is the membrane potential of the neuron, V_{Ca}= 180mV is the reversal potential for Ca^{2+} flux.

The activation (m) and inactivation (h) variables have voltage-dependences defined as follow:

$dm/dt = (m - m_\infty(V)) / \tau_m(V)$

$dh/dt = (h - h_\infty(V)) / \tau_h (V))$

Based on the study of Chemin et al. (2001), the model parameters of the artificial T conductances mimicking the human Cav3.1b, Cav3.1bc and Cav3.1be splice variants were defined with the following equations.

Cav3.1b

$m_\infty(V) = 1/(1+\exp(-(V+44.7)/3.6))$

$h_\infty(V) = 1/(1+\exp((V+65)/4.4))$

$\tau_m (V) = (\exp((V+120.9)/35.5))/2.5$ for $V<-64$

$\tau_m (V) = (1.5424 + (1/(\exp(-(V + 69.8)/4.3151) + \exp((V + 28.836)/7.498))))/2.5$ for $-64\leq V<-45$

$\tau_m (V) =(0.1672*\exp(-V/11.187)+0.4762)/2.5$ for $V\geq -45$

$\tau_h (V) =(0.0015*\exp(-V/4.8)+15.3876)/2.5$ for $V>-50$

$\tau_h (V) = (17.266 + (1/(\exp(-(V + 245.85)/33.45) + \exp((V + 34.133)/3.924))))/2.5$ for $V\leq -50$

Cav3.1be

$m_\infty(V) = 1/(1+\exp(-(V+46.3)/3.9))$

$h_\infty(V) = 1/(1+\exp((V+70.5)/4.9))$

$\tau_m (V) = (\exp((V+120.8)/34.3))/2.5$ for $V<-70$

$\tau_m (V) = (1.2952 + (1/(\exp(-(V + 78.259)/7.3366) + \exp((V + 31.786)/7.1955))))/2.5$ for $-70\leq V<-45$

$\tau_m (V) =(0.1251*\exp(-V/11.3507)+0.5088)/2.5$ for $V\geq -45$

$\tau_h (V) =(0.030629*\exp(-V/7.4)+11.3817)/2.5$ for $V>-50$

$\tau_h (V) = (23.218 + (1/(\exp(-(V + 325.58)/48.088) + \exp((V + 41.001)/3.7138))))/2.5$ for $V\leq -50$

Cav3.1bc

$m_\infty(V) = 1/(1+\exp(-(V+45)/4))$

$h_\infty(V) = 1/(1+\exp((V+71.1)/4.2))$

τ_m (V) = (exp((V+142.2)/34.7))/2.5 for V<-80

τ_m (V) = (0.9879 + (1/(exp(-(V + 115.89)/22.151) + exp((V + 35.8)/5.4062))))/2.5 for -80≤V<-45

τ_m (V) =(0.1048*exp(-V/11.7096)+0.4967)/2.5 for V≥-45

τ_h (V) =(0.01599*exp(-V/6.9)+15.5319)/2.5 for V>-50

τ_h (V) = (26.43 + (1/(exp(-(V + 397.18)/60.998) + exp((V + 42.923)/3.3646))))/2.5 for V≤-50

RT-PCR protocol

The thalamus was microdissected from 300 μm horizontal slices and immediately immersed in TRIzol® solution (Invitrogen Life Thechnologies). After tissue homogenization, total RNA was isolated according to the manufacturer` s instructions.

RT was carried out for 50 minutes at 42°C in total reaction volume of 25 μl containing 2 μg total RNA, random hexamer primers (Roche; 5 μM), the four deoxyribonucleotide triphosphates (dNTP, Qiagene; 2.5 mM of each), 20 U of ribonuclease inhibitors (Promega) and 200 U of reverse transcriptase (SuperScript II, Invitrogen). The PCR protocol was tested in final volume of 50μl containing 3μl samples of the RT reaction, 0.5 μM sense and antisense primers, 2.5 mM dNTP, 1.5 mM $MgCl_2$ and 1U HotStartTaq DNA polymerase (Qiagene) in a Gene Amp® PCR system 2700 Thermocycler (Applied Biosystems) with following cycling protocols: after 15 minutes at 94°C, 30 cycles (94°C 1min; 53°C 1min; 72°C 2min) of PCR were followed by a final elongation period of 10min at 72°C. The following sense and antisense primers were used (from 5` to 3`): Ca_V 3.1b (sense) GAGAAGGAAAGCCCAGTGCAA (5184) and, (antisense) TCTCTTCCAGCGTGATGCCCA (5495);

Ca_V 3.1bc (sense) GAAGGAATCTAATGTTGGACG (position 5215-5235),

(anti-senses) ATCTGGGGCTGCTGGTAATGT (position 5408-5428)

and Ca_V 3.1e, (sense) TGCTCTTCATCTTCATCTTCA (position 3038-3058),

(antisense) CTCGTATCTTCCCGTTTGCCG (position 3336-3356).

To investigate the presence and size of the amplified fragments, 10 μl aliquots of PCR products were separated and visualized in ethidiumbromide-stained UtraPure™ agarose (Invitrogen) gels (1%) by electrophoresis with GelPilot® 100 bp DNA molecular weight marker (Qiagene). Predicted sizes (in base pairs, bp) of PCR fragments were 311 (Ca_V 3.1b); 193 (Ca_V 3.1bc) and 298 (Ca_V 3.1e). The PCR products were sequenced several times ($n>3$) by the Beckman Coulter Genomics (France).

GenBank accession numbers. Ca_V 3.1b, AL645965, Ca_V 3.1bc, NM_001177888; Ca_V 3.1e, NM _009783.

Chemin J, Monteil A, Bourinet E, Nargeot J, Lory P (2001) Alternatively spliced alpha(1G) (Ca(V)3.1) intracellular loops promote specific T-type Ca(2+) channel gating properties. Biophys J 80:1238-1250.

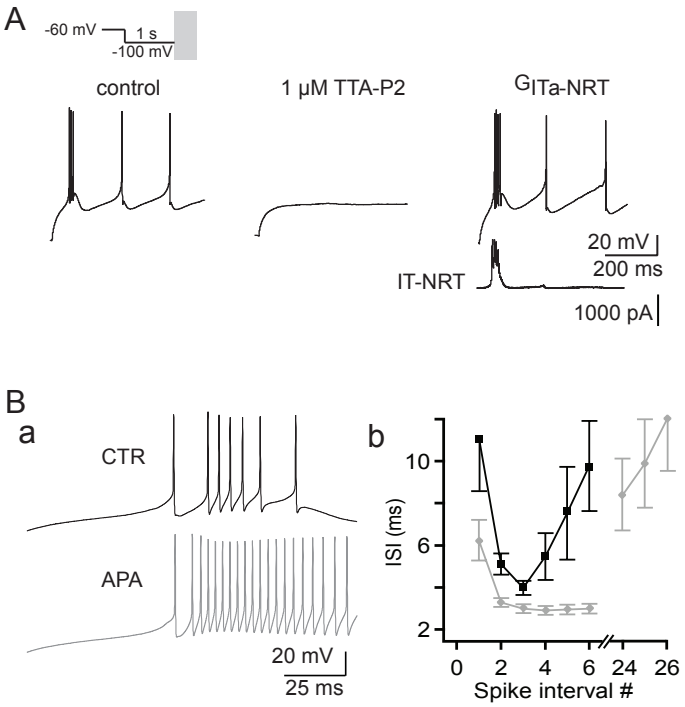

Supplemental Figure 1: The high-frequency firing associated to LTS is partially reproduced by ITa in NRT neurons.

A. LTSs were evoked at the offset of a 1s hyperpolarization to -100mV in NRT neurons from wild-type mice. Note the typical oscillatory behavior consisting of an initial LTS crowned by a burst of high-frequency action potentials followed by rhythmic discharges of action potentials. Application of 1µM TTA-P2 fully blocks this rebound activity that is fully reestablished by injecting an artificial T conductance mimicking T current (GITa-NRT) (bottom trace). **B.** Using similar protocol than in **A**, rebound bursts are evoked in NRT neurons in control condition and in presence of apamin (300nM). As shown in the typical traces in **a** and the graph of the mean ISI in **b** (n=6), block of the SK channels prolongs the burst of action potentials but the typical “accelerando-deccelerando” pattern of the burst, although reduced, is still present.

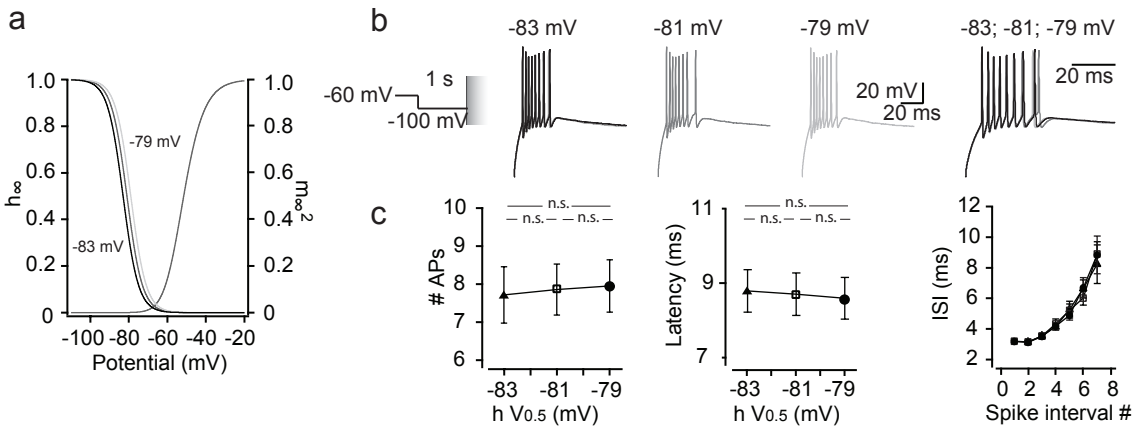

Supplemental Figure 2: Rebound bursts evoked by long hyperpolarization to -100mV are insensitive to small modifications in steady-state inactivation voltage dependencies of the T channels.

Responses of a Cav3.1$^{-/-}$ TC neuron to a 1s hyperpolarization to -100mV were successively recorded while injecting artificial T conductances displaying normal (V0.5 = -81mV), slightly hyperpolarized (V0.5 = -83mV) or depolarized (V0.5 = -79mV) activation voltage-dependence (see graph of the IV curves in **a**). As illustrated by the typical traces in **b** and quantified in c (n=7), burst firing is not modified by such slight changes in inactivation properties of the T channels.

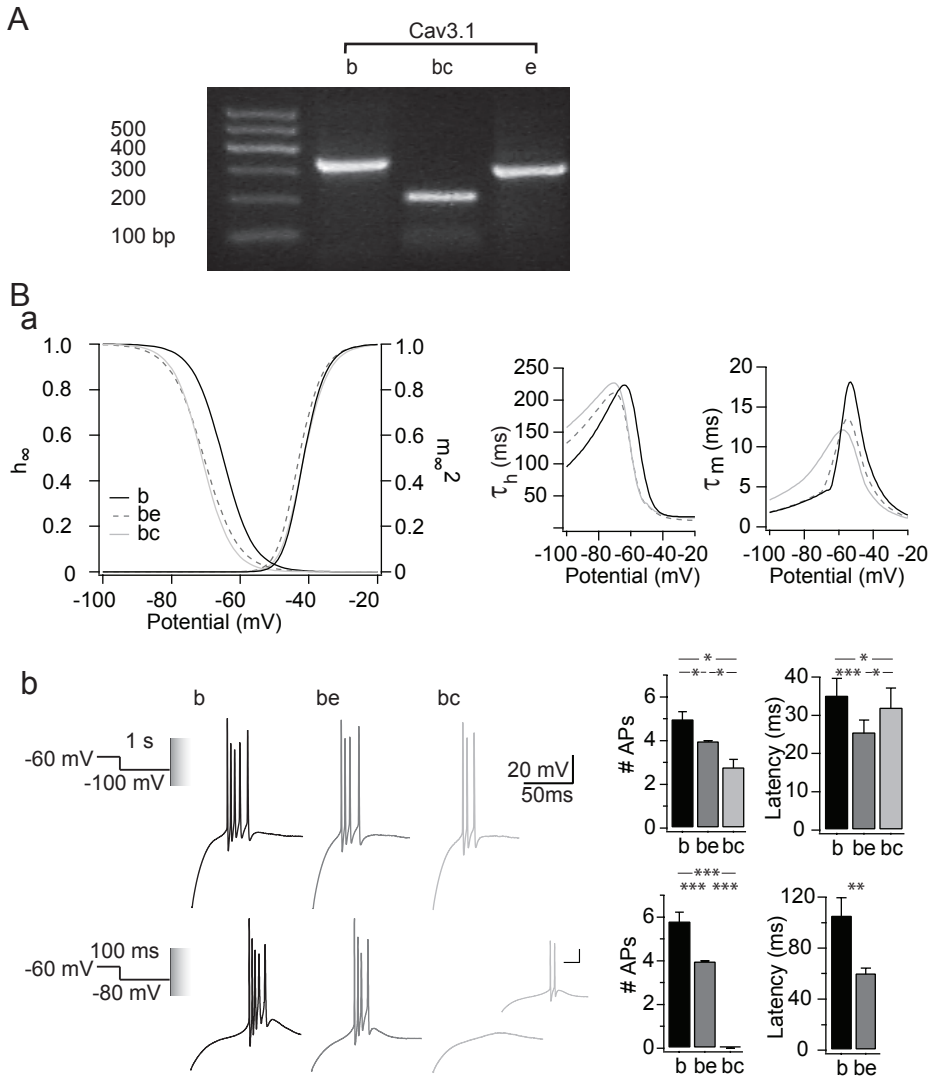

Supplemental Figure 3: The small differences in biophysical properties of the Cav3.1 splice variants expressed in TC neurons may strongly affect burst firing.

A. Representative RT-PCR data (ethidiumbromide-stained gel) showing the presence of Cav3.1b, Cav3.1bc and Cav3.1e transcripts in the adult mouse thalamus (P32, see methods). **B.a.** Graphs show the biophysical properties of artificial T conductances modeling cloned human Cav3.1b (black line), Cav3.1bc (light gray line) and Cav3.1be (dotted line) channels (see methods). Left graph: activation (m_∞^2) and steady-state inactivation (h_∞) voltage dependencies; middle and right graphs: time constant of inactivation (τh) and activation (τm) kinetics as a function of membrane potential, respectively. **b.** T conductances endowed with either the Cav3.1b, Cav3.1be or Cav3.1bc biophysical properties were injected in TC neurons at the end of a 1s hyperpolarization to -100mV (top traces) or a 100ms hyperpolarization to -80mV (bottom traces). Note the striking impact on the rebound LTS of the small changes associated to isoforms be and bc when short and weak hyperpolarization were used to evoked rebound LTS (bottom traces). Trace in inset shows that increasing the conductance by 20% did not restore excitability similar to the one observed with the b and be isoforms. Note also that although the b and be isoforms display large differences in many biophysical properties, little effects are observed on the rebound bursts evoked by both strong and weak hyperpolarization, suggesting possible compensatory mechanism between the impact of their various biophysical characteristics. The mean number of action potentials in the bursts and the latency of firing for each of the 3 isoforms are quantified in the histograms (b: n= 7; be n=7; bc: n=7). (Student paired t-test : n.s. : not significant; *: p<0.5; **: p<0.01; ***: p<0.005).